

Thin Film SOFCs with Cobalt-Infiltrated Cathodes

Keiji Yamahara^{*+}, Craig P. Jacobson⁺, Steven J. Visco⁺, Xiao-Feng Zhang⁺,

and Lutgard C. De Jonghe^{+#}

⁺Materials Science Division, Lawrence Berkeley National Laboratory,
University of California, Berkeley, CA 94720, USA

and

[#]Department of Materials science and Engineering
University of California at Berkeley
Berkeley CA 94720

Abstract

Anode-supported SYSZ [i.e. $\text{Sc}_2\text{O}_3)_{0.1}(\text{Y}_2\text{O}_3)_{0.01}(\text{ZrO}_2)_{0.89}$] thin-film solid oxide fuel cells were evaluated between 650 and 800°C. Peak power densities and power densities at cell voltages of 0.7V were 320 and 190 mW/cm², respectively, at 650°C, denoted as 320/190/650. Corresponding power densities at other temperature were 1400/1100/800, 990/640/750, and 600/360/700. At 750°C and lower the power densities and ASRs (area specific resistances) were better than those reported for an 8YSZ cell with record performance [12], while showing a smaller temperature dependence. Further performance improvements of about a factor of 2 were obtained at 650°C after infiltration of the LSM/YSZ cathodes with a cobalt solution. This improvement persisted up to about 750°C, being more pronounced at the lower temperatures. The results indicate the potential benefit of cobalt infiltration for reduced temperature SOFCs. AC measurements revealed that the majority of effect resulted from a decrease in the non-ohmic resistance of the cathode. TEM observations found ~25 nm Co_3O_4 particles in the pores of the modified LSM- composite cathodes. The AC impedance response following cobalt infiltration indicates a decrease of the effective charge transfer resistance.

PACS: Electrochemical energy conversion (84.60 D); Fuel cell (84.6 D)

Keywords: Solid oxide fuel cells; reduced temperature SOFCs; scandia-stabilized zirconia; colloidal deposition; cobalt doping

^{*}Corresponding author. Tel.: +1-510-486-5850; fax: +1-510-486-4881.
E-mail address: kyamahara@lbl.gov.

1. Introduction

Reducing the operational temperature of solid oxide fuel cells (SOFCs) from 1000°C to 600-800°C is important because it allows the use of lower-cost materials both in the stack and in the balance-of-plant. However, as the temperature is lowered, the cell performance can suffer due to the unavoidable increase in electrolyte resistance and the increased difficulty of the oxygen reduction reaction in the cathode. The development of supported thin-film SOFCs was motivated by the need to minimize the electrolyte resistance. The use of alternate, higher conductivity electrolytes, such as scandia stabilized zirconia (SYSZ), should additionally improve the low temperature performance of thin-film SOFCs [1]. Supported SYSZ thin-film SOFCs with Pt-SYSZ cathodes were examined previously [2-4]. SYSZ electrolytes, co-doped with Y_2O_3 have been considered more favorably than those of SYSZ alone, because the degradation of the ionic conductivity with time [5] can be slowed [6,7] and the microstructural stability is enhanced [8]. In addition to utilizing the high conductivity electrolytes, improvement in cathode activity at intermediate temperatures is required since the air electrode generally dominates polarization of supported thin-film SOFCs. A simple method has been reported in which the sintered composite electrodes are infiltrated with electro-catalyst precursor solutions [9]. In the present study, supported thin-film yttria co-doped SYSZ SOFCs were evaluated in between 650 and 800°C. Furthermore, the effects of cobalt post-doping by the infiltration of $La_{0.85}Sr_{0.15}MnO_3$ -SYSZ composite cathodes was examined.

2. Experimental

NiO (J. T. Baker) and [i.e. $(\text{Sc}_2\text{O}_3)_{0.1}(\text{Y}_2\text{O}_3)_{0.01}(\text{ZrO}_2)_{0.89}$] from Daiichi Kigenso Kagakukokyo] in a weight ratio of 1:1 were attritor-milled in iso-propanol, using zirconia balls. Dried mixtures were uniaxially pressed and pre-fired at 1000°C. Thin-films were formed on the NiO-SYSZ disks by colloidal deposition [10], and co-fired between 1250 and 1350°C. LSM [i.e. $\text{La}_{0.85}\text{Sr}_{0.15}\text{MnO}_3$] was synthesized by a glycine-nitrate method [11], and calcined at 1200°C. The calcined LSM powder was also attritor-milled with SYSZ in a weight ratio of 1:1. Thin cathodes, 1cm^2 , were formed on the co-fired disks, by the colloidal deposition and re-firing the assembly at 1150°C. Pt wire mesh and Pt paste were applied to both electrodes as current collectors. After the first electrochemical cell tests, the cathodes of the SOFCs were post-doped by applying 4 microliters per cm^2 of a cobalt nitrate solution [$0.5\text{g-Co}(\text{NO}_3)_2 \cdot 6\text{H}_2\text{O}$ dissolved in 1 ml of water], and then retesting the same cells. The DC current-voltage (I-V) performance was recorded with a potentiostat-galvanostat (Princeton Applied Research Model 371), between 650 and 800°C; in all tests humidified hydrogen (about 3% water) and air were used. AC impedances were measured between 0.1-10 MHz with a frequency response analyzer and a potentiostat (Solartron 1260 and 1286, respectively). Transmission electron microscopy (TEM) observations were carried out to observe the microstructures of the electrode materials before and after infiltration, using a Philips CM200 transmission electron microscope equipped with a field emission gun, and operating at 200 kV.

3. Results

A dense thin-film between a porous Ni-SYSZ and a porous LSM-SYSZ composite was

obtained by the co-firing processes, as shown in Fig.1. The electrolyte was about 27 μm thick. For this cell configuration, anode and cathode microstructures and their activity depended significantly on the electrolyte/Ni-SYSZ co-firing temperatures between 1250-1350°C, and the subsequent cathode forming temperatures between 1100-1200°C. One cell, co-fired at 1300°C followed by the cathode forming at 1150°C showed the best performance in this set, Fig. 2, with peak-power (mW/cm^2) / power (mW/cm^2) at 0.7 V / temperature (°C) of 1400/1100/800, 990/640/750, 600/360/700, and 320/190/650. Table 1 compares the ASRs (area specific resistances), ohmic resistances and their apparent activation energies with those of anode supported 8YSZ cells reported previously [1, 12, 13]. The ASRs were taken to be defined by the cell voltage difference between open circuit and at a current density of 1 A/cm^2 , while the ohmic resistance was determined from the high frequency intercepts in Cole-Cole plots. The peak power density of cell at 800°C was lower than the 1.9 mW/cm^2 reported for the best 8YSZ-based cells. However, it should be noticed that the temperature dependence of power density was smaller for the YSZ cell. The peak power density was, thus, significantly higher for the SYSZ cell at 750°C and below. This advantage was also observed for the ASRs, and indicates a benefit in using SYSZ instead of 8YSZ, especially for low temperature operation. Additionally, the apparent activation energy calculated for the ASR was lower than that for the ohmic resistance. Thus, non-ohmic contribution associated with the cathode becomes comparatively more significant at lower temperatures.

The effect of cobalt infiltration into the LSM-SYSZ cathode was examined. It was found, Figs. 3 and 4, that at 650°C, the cobalt infiltration improved the peak power densities and the power densities at 0.7 V by as much as a factor of 1.8 and 2.2,

respectively. The improvement in power density was observed over the temperature range of 650-750°C, and was more significant at lower temperatures. Additionally, it can be seen in Fig. 4 that the magnitude of the improvement, while evident in all cases, varied from cell to cell, probably because of some difference in microstructures of the cathodes. AC impedance measurements indicated that the improvement by the cobalt infiltration was mainly due to a reduction in the cathode non-ohmic resistance (especially in a low frequency part), with a slight reduction in ohmic-resistance, as seen in Cole-Cole plots of Fig. 5. TEM observations, Fig. 6, showed the presence of nano-particles with an average size of 25 nm in the pores of infiltrated LSM-SYSZ composites after heating to the operational temperature. The nano-particles were identified as Co_3O_4 , and no other reaction products were detected by X-ray diffraction or TEM. The improvement by cobalt infiltration might be attributed to enhancement of surface processes on the LSM itself, or to the creation of new oxygen reduction sites and additional triple phase boundaries with the cobalt spinel particles. The strong modification of the low frequency part of the AC impedance response following cobalt infiltration points to a decrease of the effective charge transfer resistance. However, the current data or available modeling work in the literature, do not allow for unambiguous conclusions about details of the mechanisms that determine the enhanced cathode performance.

4. Conclusion

Supported SYSZ thin-film electrolyte SOFCs demonstrated high performance of 1400/1100/800, 990/640/750, 600/360/700, and 320/190/650¹. At 750°C and lower temperatures the densities and ASRs were significantly better, with less temperature dependences than those previously reported for the best 8YSZ-based cells [12]. This indicates that using SYSZ instead of 8YSZ is beneficial, especially for low temperature operation. Cobalt infiltration was accomplished by contacting the LSM-SYSZ cathode after fabrication with a cobalt nitrate solution. The power densities at peak and at 0.7 V were improved by as much as 1.8 and 2.2 times, respectively, at 650°C. This improvement was observed over the temperature range 650-750°C, and was more pronounced at the lower temperatures indicating the potential benefit of the cathode cobalt infiltration for reduced temperature SOFCs. AC impedance measurements showed a strong reduction in non-ohmic resistance, and a slight one in ohmic resistance. TEM revealed the presence of ~25 nm diameter Co₃O₄ particles in the pores of the LSM-SYSZ composite cathodes. The strong modification of the low frequency part of the AC impedance response following cobalt infiltration points to a decrease of the effective charge transfer resistance.

¹ this notation means: peak-power in mW/cm² /power at 0.7 V in mW/cm² /temperature of operation in °C

Acknowledgements

This work was supported by the U.S. Department of Energy, National Energy Technology Laboratory. The authors are grateful to Daiichi Kigenso Kagakukogyo for supplying SYSZ powder. Andrés Leming and Tal Z. Sholklapper are thanked for assistance in the experiments. Part of this work was made possible through the use of the National Center for Electron Microscopy facility at the Lawrence Berkeley National Laboratory.

References

1. Steven J. Visco, Craig P. Jacobson, and Lutgard C. De Jonghe, in *SOFC VI*, S.C. Singhal and M. Dokiya, Editors, **PV 99-19**, p. 861, The Electrochemical Society Proceedings Series, Pennington, NJ, (1999).
2. M. Dokiya, Solid State Ionics, **152-153** (2002) 383.
3. K. Kobayashi, I Takahashi, M. Shiono and M. Dokiya, Solid State Ionics, **152-153** (2002) 591.
4. Z. Cai, T.N. Lan, S. Wang and M.Dokiya, Solid State Ionics, **152-153** (2002) 583.
5. S.P.S Badwal, F.T. Ciacchi, J. Drennan and S. Rajendran, Solid State Ionics, **109** (1998) 167.
7. F.T. Ciacchi and S.P.S Badwal, J. Eur. Ceram. Soc.,7 (1991) 197.
8. Y. Arachi, O. Yamamoto, Y. Takeda and N. Imanishi, Denki Kagaku, 64 (1996) 638.
9. S.A. Wallin, U.S. Pat. No. 6017647, January 25 (2000).
10. S.J. Visco, C.P. Jacobson and L.C. De Jonghe, U.S. Pat. No. 6458170, October 1 (2002).
11. L.A. Chick, L.R. Pederson, G.D. Maupin, J.L. Bates, L.E. Thomas, and G.J. Exarhos, Mater. Lett., **10** (1-2), (1990) 6.
12. S. de Souza, S.J. Visco, L.C. De Jonghe, in Proceeding of the Second European Solid Oxide Fuel Cell Forum, edited by B. Thorstensen, Vol. 2, 677 (1996).
13. S. de Souza, S.J. Visco, L.C. De Jonghe, J. Electrochem. Soc., 144 (3), (1997) L35.

Table 1 Comparison of cell performance and apparent activation energy between the present anode supported SYSZ cell and anode supported 8YSZ cells [1,12,13].

Fig.1 SEM micrograph of the cross-section of a supported SYSZ thin-film cell.

Fig.2 Cell voltage and power density as a function of current density for a supported SYSZ thin-film cell at the temperatures of 800, 750, 700, and 650°C. The fuel cell anode/electrolyte was co-fired at 1300°C, while the cathode was applied and sintered at 1150°C.

Fig. 3 Cell voltage and power density as a function of current density before and after cobalt infiltration. The electrolyte/anode was co-fired at 1300°C, and the cathode, prepared from SYSZ powder calcined at 1200°C, was applied and sintered at 1150°C.

Fig.4 Temperature dependence of peak power density and power density at the cell voltage of 0.7V before and after cobalt infiltration for different two cells. (a) The fuel cell was the same as the cell in Fig. 3. (b) The electrolyte/anode was co-fired at 1350°C, and the cathode was then applied and sintered at 1150°C.

Fig. 5 Cole-Cole plots for the same cell as (a) in Fig. 4 and the one in Fig. 3 before and after the cobalt infiltration into the LSM-SYSZ cathode. Triangles and squares in the

plots indicate frequencies of 10 k, 1 k, 100, 10, 1 and 0.1 Hz from the left to the right.

High frequency intercepts were 0.143 (0.137), 0.183 (0.168), and 0.287 (0.221) Ωcm^2 before (and after) infiltration at 750, 700 and 650°C, respectively.

Fig. 6 TEM pictures for an LSM-SYSZ composite before (a) and after cobalt infiltration (b) heat-treated up to 650°C. Nano-size Co_3O_4 is marked.

Table 1

Temperature (°C)	Peak power density (W/cm ²)			ASR at 1A/cm ² (Ω cm ²)		Ohmic resistance (Ω cm ²)	
	Present	de Souza[12]	Visco[1]	Present	de Souza[12]	Present	Souza[13]
800	1.4	1.9		0.30	0.26	0.085 ^a	0.1 ^b
750	0.99	0.58	0.89	0.43	0.54	0.12 ^a	
700	0.60	0.35	0.30	0.59	0.96	0.19 ^a	
650	0.32	0.14		0.79	2.0	0.29 ^a	
Apparent activation energy (eV)				0.55	1.1	0.70	

^a The values were determined by the low intercept in Cole-Cole plots of AC impedance.

^b The values were determined by a current-interrupt technique.

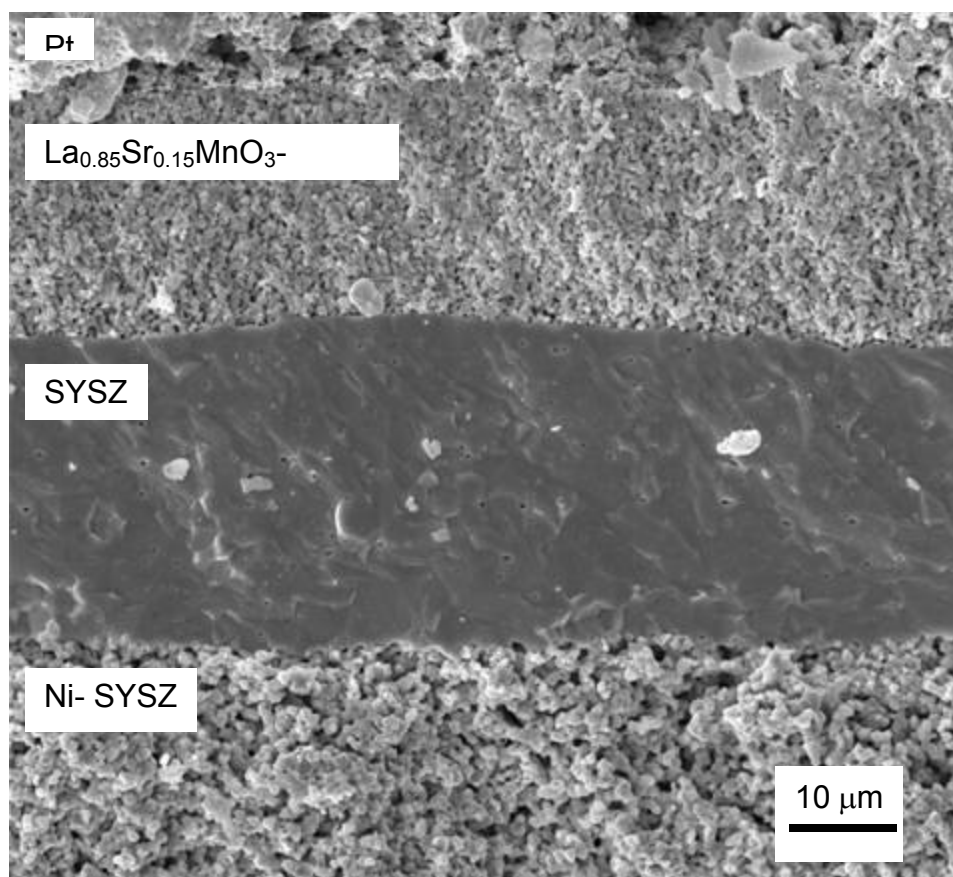


Fig. 1

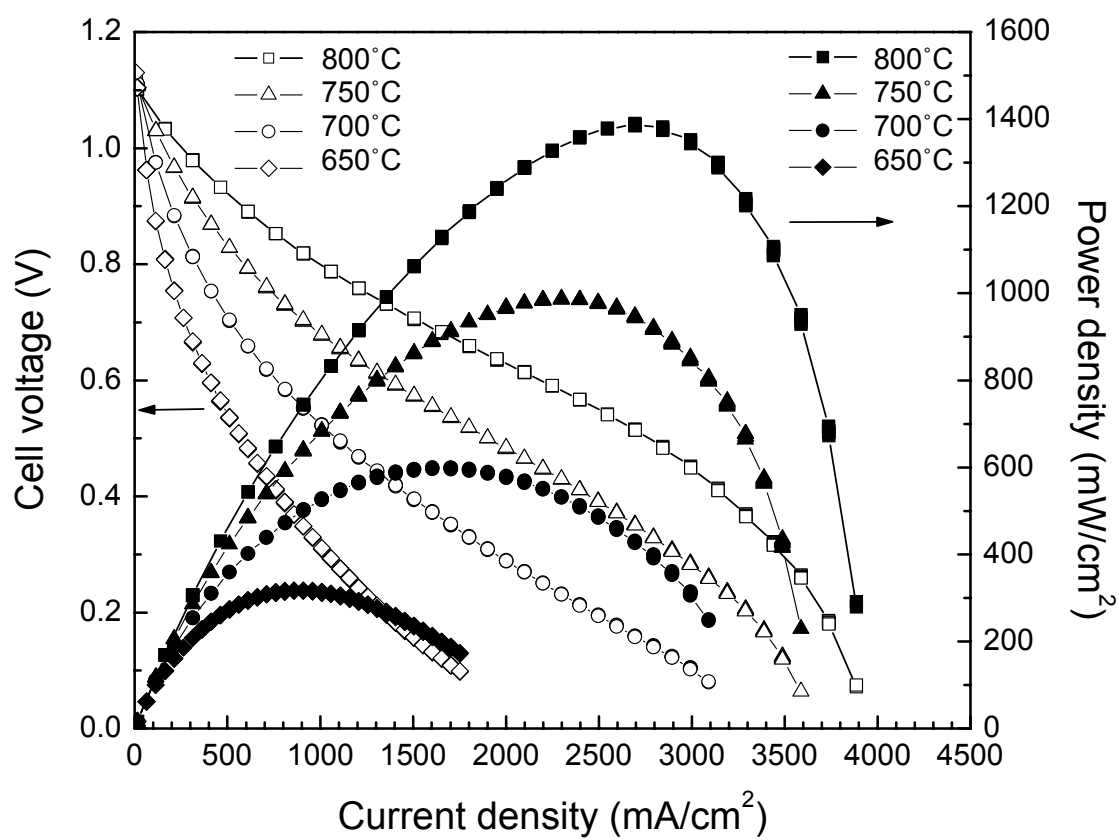


Fig. 2

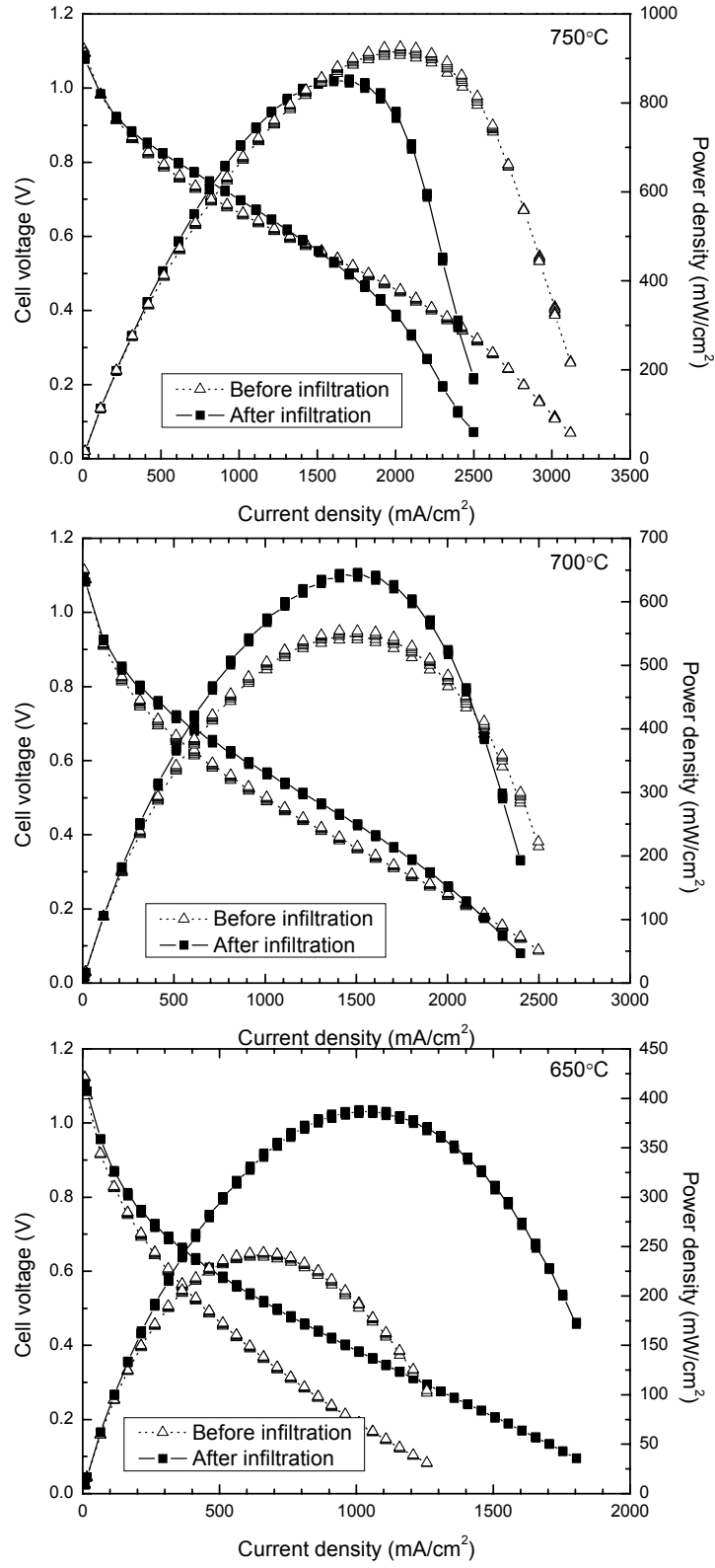
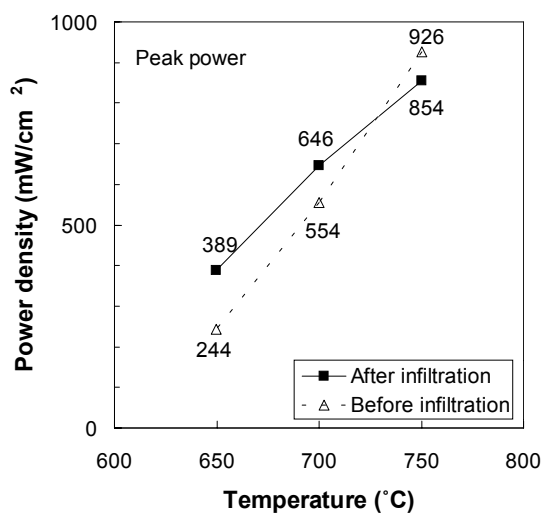
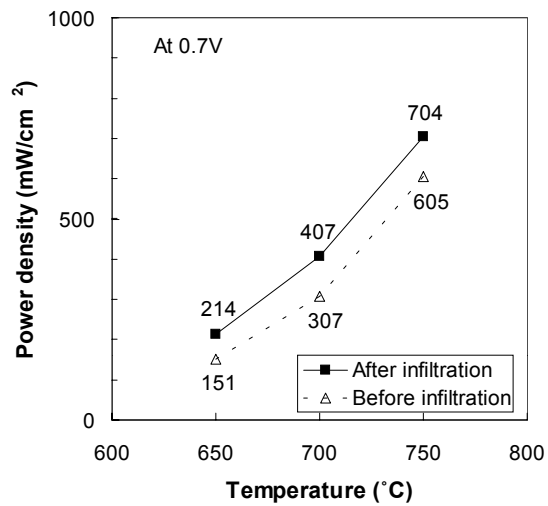


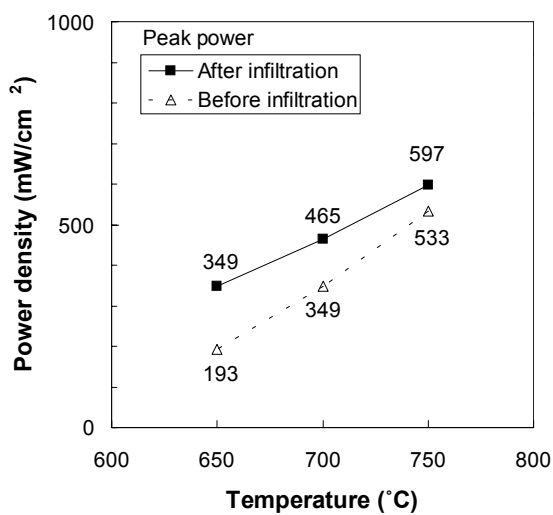
Fig. 3



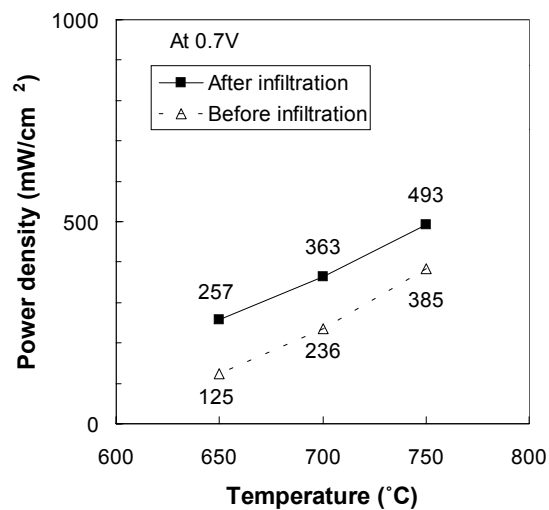
(a)



(a)



(b)



(b)

Fig. 4

Fig. 5

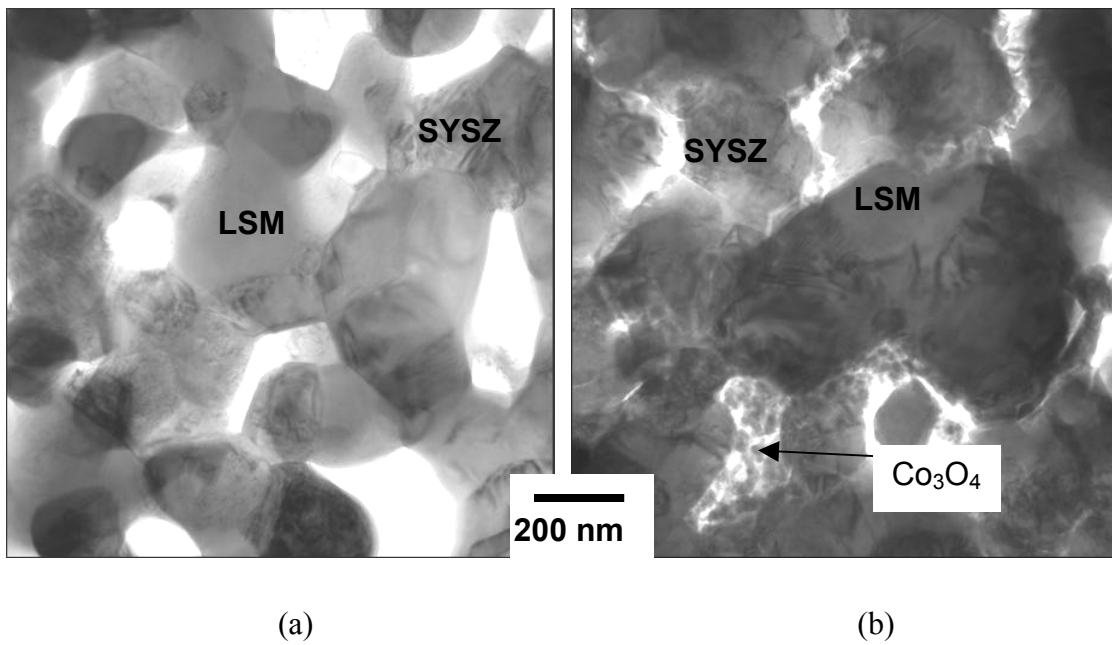


Fig. 6